Interobserver Delineation Variation Using CT versus Combined CT + MRI in Intensity-Modulated Radiotherapy for Prostate Cancer

Geert M. Villeirs[1], Koen Van Vaerenbergh[2], Luc Vakaet[2], Samuel Bral[2], Filip Claus[2], Wilfried J. De Neve[2], Koenraad L. Verstraete[1], Gert O. De Meerleer[2]

Purpose: To quantify interobserver variation of prostate and seminal vesicle delineations using CT only versus CT + MRI in consensus reading with a radiologist.
Material and Methods: The prostate and seminal vesicles of 13 patients treated with intensity-modulated radiotherapy for prostatic adenocarcinoma were retrospectively delineated by three radiation oncologists on CT only and on CT + MRI in consensus reading with a radiologist. The volumes and margin positions were calculated and intermodality and interobserver variations were assessed for the clinical target volume (CTV), seminal vesicles, prostate and three prostatic subdivisions (apical, middle and basal third).
Results: Using CT + MRI as compared to CT alone, the mean CTV, prostate and seminal vesicle volumes significantly decreased by 6.54%, 5.21% and 10.47%, respectively. More importantly, their standard deviations significantly decreased by 63.06%, 62.65% and 44.83%, respectively. The highest level of variation was found at the prostatic apex, followed by the prostatic base and seminal vesicles.
Conclusion: Addition of MRI to CT in consensus reading with a radiologist results in a moderate decrease of the CTV, but an important decrease of the interobserver delineation variation, especially at the prostatic apex.

Key Words: Prostate neoplasms · Therapeutic radiology · Computed tomography (CT), comparative studies · Magnetic resonance (MR), comparative studies · Diagnostic radiology · Observer performance · Conformal radiotherapy

Strahlenther Onkol 2005;181:424–30
DOI 10.1007/s00066-005-1383-x

Quantifizierung der Interobserver-Variation im CT im Vergleich zur Kombination CT und MRT bei intensitätsmodulierter Strahlentherapie

Ziel: Quantifizierung der Interobserver-Variation bei der Abgrenzung von Prostata und Samenblasen im CT im Vergleich zur Kombination CT und MRT nach einer Konsensusbefundung mit einem Radiologen.
Material und Methodik: Die Prostata und die Samenblasen von 13 Patienten, die für eine intensitätsmodulierte Strahlentherapie wegen Adenokarzinoms der Prostata vorgesehen waren, wurden retrospektiv im CT und mit der Kombination CT und MRT durch drei Strahlentherapeuten nach einer Konsensusbefundung mit einem Radiologen abgegrenzt. Volumen und Randpositionen wurden berechnet und die Intermodalitäts- bzw. Interobservervariationen für das klinische Zielvolumen (CTV), die Samenblasen, die Prostata und drei Prostatasegmente (apikales, mittleres und basales Drittel) beurteilt.
Ergebnisse: Mit der Kombination von CT und MRT verringerte sich im Vergleich zur alleinigen CT der Mittelwert für das CTV, Prostata- und Samenblasenvolumen signifikant um 6,54%, 5,21% und 10,47%. Von größerer Bedeutung war die signifikante Abnahme der Standardabweichungen um 63,06%, 62,65% und 44,83%. Die höchste Variation wurde im Apex der Prostata festgestellt, gefolgt von der Basis der Prostata und den Samenblasen.
Schlussfolgerung: Die Kombination von CT und MRT nach Konsensus mit einem Radiologen resultiert in einer bedeutenden Abnahme der Interobservervariation bei der anatomischen Abgrenzung, insbesondere im Bereich des Apex der Prostata, und zusätzlich in einer moderaten Verringerung des CTV.

Schlüsselwörter: Prostataneoplasien · Strahlentherapie · Computertomographie (CT), vergleichende Studien · Kernspintomographie (MRT), vergleichende Studien · Diagnostische Radiologie · Beobachterleistung · Konformale Strahlentherapie

[1] Department of Radiology, Ghent University Hospital, Gent, Belgium,
[2] Department of Radiotherapy, Ghent University Hospital, Gent, Belgium.

Received: October 19, 2004; accepted: April 26, 2005

Introduction

Several authors have demonstrated that a higher radiation dose to the prostate is associated with improved local tumor control [12, 20, 25, 27], but at the price of a latent increase in normal tissue complication rate [14]. With conformal or intensity-modulated radiation therapy (IMRT), it is possible to increase the radiation dose to the target volume while minimizing the dose to the surrounding normal tissues, by applying tightly constricted isodose lines around the target, thereby minimizing the risk of acute and late complications [2, 5, 8, 10, 13, 16, 17, 23]. The latter statement only holds true when these isodose lines are adequately placed around the target volume and therefore, accurate delineation of the clinical target volume (CTV) and surrounding tissues is crucial. These delineations are usually performed by radiation oncologists on CT images, in part because CT can easily produce tissue electron density values (calculated from Hounsfield units), which are required for dose calculations and to account for tissue inhomogeneities within the treatment volume [15]. Compared to CT, more anatomic information can be derived from MRI due to its multiplanar imaging capability and its higher soft-tissue contrast on T2-weighted images, resulting in detailed visualization of both the prostate and periprostatic structures [19]. This advantage can be employed indirectly by using MRI information to improve the delineation accuracy on CT images or by direct delineation on the MR images, using image segmentation and image registration or correlation to account for the lack of tissue electron density values on MRI [11, 15]. However, due to the complexity of interpreting MRI without the helping hand of a radiologist, its advantage might be offset to some extent.

The aim of our study was to assess whether the additional anatomic information derived from MRI in consensus reading with a radiologist could decrease the interobserver variation of prostate and seminal vesicle delineations on CT images, and in the given case, to quantify this effect with reference to prostatic anatomy.

Material and Methods

Between April 2000 and April 2003, 187 patients were admitted to the Radiotherapy Department of Ghent University Hospital, Belgium, to receive primary IMRT for histologically proven localized adenocarcinoma of the prostate. Out of this group, 13 patients (mean age 68 years, range 57–74 years) were randomly selected for retrospective delineation of the prostate and seminal vesicles by three radiation oncologists (F.C., S.B., L.V.), initially on CT images only and subsequently with the addition of MRI data in consensus reading with a radiologist specialized in pelvic imaging (G.M.V.). At the start of the study, all radiation oncologists received a supplemental 1-day training in pelvic radio-anatomy (CT and MRI). Observers 1 and 2 had < 5 years of experience in pelvic target delineation, whereas observer 3 had > 10 years of experience.

All CT data were acquired on a helical CT scanner (Siemens Somatom 4+, Siemens, Erlangen, Germany) as previously described [5]. The patients were instructed to drink 750 ml of dilute contrast medium (30 ml Gastrografin® [Schering, Berlin, Germany] in 720 ml water) the evening before and the morning of the CT scan procedure to increase the visibility of the small bowel and sigmoid colon. Approximately 30 min before the CT scan procedure, all patients received a rectal laxative (Microlax®, Sanofi-Winthrop, Colomiers, France) and were asked to drink an additional 300 ml of water. This procedure ensures a comfortably filled bladder during treatment, in an attempt to keep as much small bowel loops away from the treatment field as possible [6, 26]. To further improve visualization of the bladder, 100 ml of intravenous iodinated contrast medium (Ultravist®, Schering) was administered 10 min prior to the CT scan procedure [24]. The CT data consisted of 10 mm thick contiguous sequential slices obtained in the supine position from the level of the umbilicus to a level 10 cm caudal to the testes. Additional data on prostate, seminal vesicles and surrounding tissues were obtained using 2 mm (n = 5) or 5 mm (n = 8) thick contiguous slices from the superior border of both femoral heads to the distal border of the ischial tuberosity. Scanning parameters were 120 KV voltage and 185 mAs tube current, 750 ms rotation time, 2–10 mm collimation and table feed per rotation. All patients were scanned in the treatment position, supine on a flat table and legs gently bent on a knee fix (Sinmed Kneefix cushion, Cablon Medical, Leusden, The Netherlands).

Within 1–6 days following the CT scan, an MRI study was obtained in all patients on a 1-T MRI scanner (Magnetom Expert, Siemens), using a pelvic phased-array coil. 5-mm transverse, sagittal and coronal T2-weighted turbo-spin echo images (TR/TE 4,000/99 ms, two signal averages, no interslice gap, 25- to 40-cm field of view [FOV], and matrix size of 330 × 512) of the pelvis were obtained. Approximately 30 min before the MRI scan procedure, all patients received a rectal laxative (Microlax®, Sanofi-Winthrop) and were asked to drink 300 ml of water, in order to attain a comfortably filled bladder. All patients were scanned in the same treatment position as described above, with the pelvis positioned in the isocenter of the magnet.

Both the CT and MR data were available on hard copy and the CT data were digitally transferred to a Pinnacle^3 computer workstation (ADAC, Philips Medical Systems, Best, The Netherlands). On every CT slice, contouring of the prostate and seminal vesicles was performed, first by a radiation oncologist without additional MRI data nor the help of a radiologist. After an interval of at least 2 weeks, the same set of images was again delineated in a randomized order by the same radiation oncologist and with the addition of MRI data in consensus reading with the radiologist, by transferring the MRI information visually to the CT data set on the computer workstation, without image registration nor fusion. Since the use of an endorectal coil would interfere with prostate shape and position, only images acquired with pelvic phased-array coil were used to transfer data. All consensus readings by the

radiologist were performed in a randomized order and with an interval of at least 1 month between each set of consensus readings.

The surface of the delineated prostate and seminal vesicles on each slice was calculated using the treatment planning system and this surface was multiplied with the interslice distance, yielding the respective volume in each slice. Summation of all these volumes yielded the total prostate and seminal vesicle volume and the sum of these two volumes yielded the CTV. Furthermore, the prostate was arbitrarily divided into three parts: an apical, middle and basal third. This definition was based on the prostate volume averaged from the MRI-based volumes of the three observers. The total number of slices corresponding to this averaged volume was divided by 3. The lower, middle and upper n/3 slices were considered the apical, middle and basal third, respectively. On each slice, the average volume and standard deviation (SD) of the three observer measurements were calculated. Subsequently, the mean of these averages and their SDs were calculated for both CT- and MRI-based volumes of the CTV, prostate gland, basal, middle and apical third and seminal vesicles. Comparisons between CT- and MRI-derived values (means or SD) were represented in percentage decrease, defined as $(x_{CT}-x_{MRI})/x_{CT}$; negative values indicated that the MRI-derived value was larger than the corresponding CT-derived value. Also, the dimensionless coefficient of variation (%), defined as the ratio between the SD and the mean, was calculated to measure the relative scatter in data with respect to the mean.

To quantify the modality-related delineation uncertainty of the observers, we calculated the delineation uncertainty ratio by slightly modifying a method introduced by Rasch et al. [21]. It is defined as the ratio between the actually delineated volume on a given modality (CT or MRI) and the CT/MRI intersection volume (the volume that was jointly delineated on both CT and MRI). A large ratio means that a large amount of the actually delineated volume is discordant with the CT/MRI intersection volume (high degree of uncertainty), whereas a ratio of 1 means that the actually delineated volume equals the intersection volume (low uncertainty). In two patients, however, the CT-based apical prostatic volume was very small because of discordant delineation in the lowermost aspect of the prostate, leading to an inappropriately small intersection volume and hence extremely outlying uncertainty ratios on MRI. These ratios were therefore excluded from further analysis.

Besides variation in delineated volumes, variations in the position of the anterior, posterior, right, left, superior and inferior margins of the prostate were assessed and broken down into the three prostatic thirds. A coordinate system was constructed through the interobserver mean center of gravity (COG) of the prostate, as determined on the MRI images. The z-axis (parallel to the body axis and perpendicular to the scan plane) was defined at the intersection of a sagittal and a coronal plane through the COG. On each CT slice, the distance to the z-axis (in mm) of the anterior and posterior prostatic border in the sagittal plane and of the right and left prostatic border in the coronal plane to the z-axis was calculated. Furthermore, the distance between the superior and inferior border of the prostatic base and apex was determined by counting the number of delineated slices and multiplying it with the interslice distance. To compare CT- and MRI-derived differences, the MRI-derived distances were subtracted from the corresponding CT-derived distances, a negative number indicating a larger MRI-derived distance and vice versa. For the anteroposterior and mediolateral directions, the mean difference and SD of the three observer measurements per prostatic third were calculated.

Differences of the mean were considered in three categories: intramodality interobserver, intermodality intraobserver and intermodality all-observer variation. Statistical significance testing of means in the first category was performed using the one-way analysis of variance for independent samples (ANOVA) and Student's paired t-test in the other categories. The null-hypothesis was rejected if $p < 0.05$. Correlations were analyzed using Pearson's product moment correlation coefficient (r).

Results

The mean delineated volumes of the CTV, prostate, seminal vesicles, prostatic base, midprostate and prostatic apex per modality (CT or MRI) and per observer are shown in Figures 1 and 2. We found no statistically significant intramodality interobserver differences of these mean delineated volumes both on CT or MRI (one-way ANOVA), indicating that any intermodality differences could not be attributed to deviant delineations by one of the observers. Equally, no statistically significant intramodality interobserver differences of the position of the margins were found (one-way ANOVA).

The addition of MRI led to a significant intermodality intraobserver reduction of all delineated volumes in observer 1, especially at the apical third (paired Student's t-test). Interestingly, the delineated prostate volume on CT was slightly smaller than on MRI in the most experienced observer, largely because of an apparent underestimation of the middle third volume.

Overall, we found a significant intermodality all-observer reduction of the mean delineated CTV volumes of 6.54%, consisting of a 5.21% reduction of the prostate mean volume and a 10.47% reduction of the seminal vesicle mean volume (Table 1). Within the prostate, we observed a nonsignificant 3.10% reduction of the basal third mean volume, a significant 3.22% reduction of the middle third mean volume and a near-significant ($p = 0.0504$) 14.16% reduction of the apical third mean volume (Student's paired t-test). There was no correlation between the magnitude of MRI-induced volume reduction and the actual volume of the CTV, prostate, basal third, middle third, apical third or seminal vesicles (Pearson's correlation coefficients $r = 0.03$, –0.01, –0.16, –0.08, 0.27 and –0.09, respectively; all p-values > 0.05).

There was a significant decrease of the intermodality all-observer mean SDs. When MRI was used in addition to CT, we found a 63.06% reduction of the SD around the mean CTV volume, consisting of a 62.65% reduction of the SD around the mean prostate volume and a 44.83% reduction of the SD around the mean seminal vesicle volume (Table 1). Within the prostate, we observed a reduction of the mean SD around the mean volumes of the basal, middle and apical thirds of 33.69%, 66.24% and 53.62%, respectively. All these reductions were highly statistically significant (Student's paired t-test). When the coefficient of variation was calculated (SD/mean), a particularly high variation was found on CT at the level of the apical third (Table 1).

A weak correlation was found between the magnitude of MRI-induced mean SD reduction and the actual volume of the prostate (Pearson's correlation coefficient $r = 0.60$; $p < 0.05$). The other correlations (CTV, basal third, middle third, apical third and seminal vesicles) were insignificant (Pearson's correlation coefficients $r = 0.46$, 0.16, 0.37, 0.34 and –0.41, respectively; all p-values > 0.05).

Delineation uncertainty ratios on CT and MRI are presented in Table 2. Clearly, the largest ratios are found on CT delineations and at the apical third. Overall, significant reductions in delineation uncertainty were observed in the CTV and the seminal vesicles. Within the prostate, a significant reduction was only observed at the apical third.

The mean distance between the CT- and MRI-derived prostatic margins are represented in Table 3. In the transverse plane, all margins were further away from the z-axis on CT than on MRI, except on the right side. On the other hand, the superior and inferior margin on MRI was further away from the COG than on CT. The mean SD of the distance of the prostatic margins to the z-axis or COG are represented in Table 4. All SDs significantly decreased with the use of MRI, except at the anterior aspect of the apical third and the left and superior side of the basal third (Student's paired t-test).

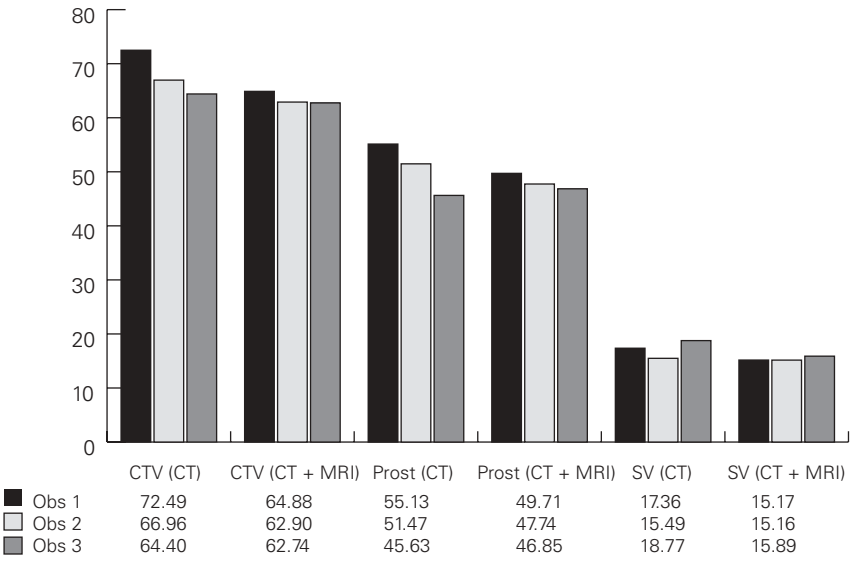

Figure 1. Mean delineated volumes of the CTV, prostate and seminal vesicles on CT and MRI for each observer (in ml).

Abbildung 1. Mittleres CTV, Prostata- und Samenblasenvolumen im CT und MRT für jeden Beobachter (in ml).

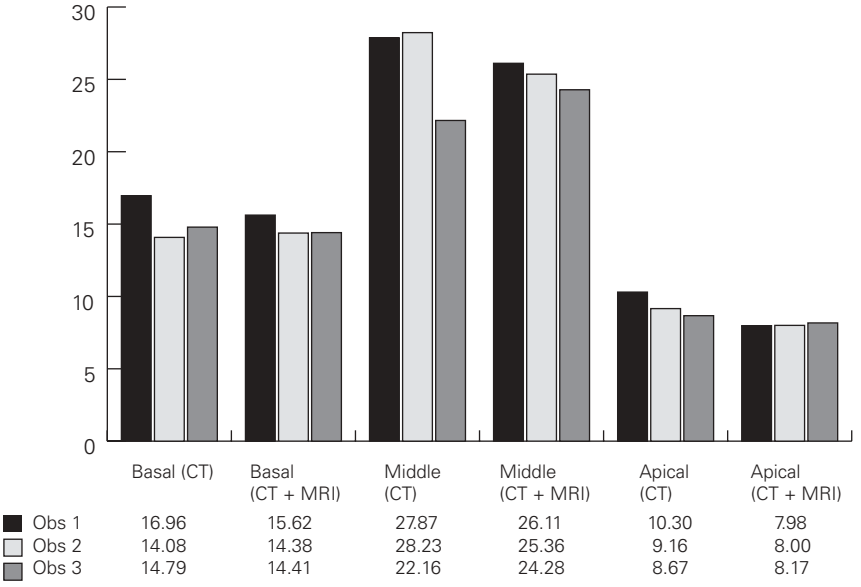

Figure 2. Mean delineated volumes of the basal, middle and apical prostatic third on CT and MRI for each observer (in ml).

Abbildung 2. Mittleres Volumen des basalen, mittleren und apikalen Prostatadrittels im CT und MRT für jeden Beobachter (in ml).

Discussion

The organ-discriminating power on CT examinations is much lower than on MRI examinations. CT is able to discriminate various tissues based solely on differences of their attenuation coefficients [11]. Since the prostate, rectal and bladder wall,

Table 1. Intermodality all-observer means and standard deviations of delineated volumes (in ml). CTV: clinical target volume.

Tabelle 1. Intermodalitätsmittelwerte und Standardabweichungen der ermittelten Volumina für alle Beobachter (in ml). CTV: klinisches Zielvolumen.

	Means			Standard deviations			Coefficient of variation	
	CT	MRI	% reduction	CT	MRI	% reduction	CT	MRI
CTV	67.95	63.50	6.54*	8.21	3.03	63.06*	12.09%	4.78%
Prostate	50.74	48.10	5.21*	7.43	2.77	62.65*	14.64%	5.77%
• Basal third	15.28	14.80	3.10	2.34	1.55	33.69*	15.34%	10.50%
• Middle third	26.09	25.25	3.22*	3.72	1.26	66.24*	14.26%	4.98%
• Apical third	9.38	8.05	14.16	2.88	1.34	53.62*	30.73%	16.60%
Seminal vesicles	17.21	15.41	10.47*	2.47	1.36	44.83*	14.36%	8.85%

*significance at $p < 0.05$ (paired t-test)

levator ani muscle and penile bulb all have similar attenuation coefficients, they cannot readily be discriminated on CT images, resulting in potentially significant inaccuracies. Furthermore, CT is only able to acquire images in the transverse plane. Due to partial volume averaging (which enlarges with increasing slice thickness), additional inaccuracies may occur. Conversely, MRI can demonstrate and characterize soft tissues by providing superb soft-tissue contrast on T2-weighted images, and by allowing direct multiplanar image acquisition without loss of spatial resolution [11]. MRI can therefore show in much more detail the prostatic margins in any direction, leading to more accurate delineations.

We found a significant decrease of the CTV volume (6.54%) when MRI was used in addition to CT. More importantly, the mean SD, coefficient of variation and uncertainty ratio decreased, meaning that the overall interobserver agreement of delineation improved.

Table 2. Delineation uncertainty index. CTV: clinical target volume.

Tabelle 2. Unsicherheitsindex der ermittelten Volumina. CTV: klinisches Zielvolumen.

	CT	CT + MRI
CTV	1.16*	1.09*
Prostate	1.16	1.10
• Basal third	1.13	1.10
• Middle third	1.10	1.07
• Apical third	1.40*	1.20*
Seminal vesicles	1.20*	1.07*

*significance at $p < 0.05$ (paired t-test)

Table 3. Intermodality all-observer mean difference between CT- and MRI-derived prostatic margin positions (in mm). Negative values indicate that the MR-derived margin is further from the z-axis or center of gravity than the CT-derived margin.

Tabelle 3. Mittlere Intermodalitätsdifferenz zwischen den computer- und kernspintomographisch bestimmten Randpositionen der Prostata für alle Beobachter (in mm). Negative Werte zeigen, dass der kernspintomographisch ermittelte Seitenrand sich weiter entfernt von der z-Achse oder dem Gravitätszentrum befindet als der computertomographisch ermittelte Seitenrand.

	Anterior	Posterior	Right	Left	Superior/inferior
Basal third	0.8	0.1	–0.3	0.3	–0.3
Middle third	0.9	0.6	–0.1	0.4	–
Apical third	1.3	1.1	0.8	1.1	–1.5

The apical third of the prostate is the most problematic area for accurate delineation on CT, and a high coefficient of variation and uncertainty ratio were observed in our study. The main reasons for this inaccuracy are the susceptibility of CT to partial volume averaging in the transverse plane and the inability of CT to discriminate the prostatic apex from surrounding tissues (levator ani muscle, rectum, distal urethral sphincter and fibrous tissue in the urogenital diaphragm), because they all have similar attenuation coefficients. Furthermore, the fibromuscular and glandular elements at the prostatic apex diffusely intermingle with one another, with the adjoining external urethral sphincter and surrounding fibrous tissue, further adding to the delineation uncertainty [3]. It is therefore virtually impossible to ascertain which slice represents the lowermost part of the prostate, which was clearly illustrated by the high SD around its mean craniocaudal distance (stated differently: a high interobserver variation in the number of delineated slices). Because of its better soft-tissue contrast and its direct multiplanar image acquisition capability, MRI can more reliably show the boundary between the high signal-intensity peripheral zone tissue and the low signal-intensity levator ani muscle, rectum, distal urethral sphincter and fibrous tissue in the urogenital diaphragm. Compared to the mean CT delineation, the MRI delineation is somewhat narrower in the anteroposterior and mediolateral direction, but taller in the superior-inferior direction. More importantly: for an almost equal delineated apical third volume, we actually saw a halving of the mean SD around this mean and of the coefficient of variation and a considerable decrease of the uncertainty ratio. Except for the anterior border, there was a significant near-halving of the mean SD around the mean position of the apical borders, all illustrating the impact of better visualization of the apical tissue on MRI and corroborating previous findings at other institutions [1, 4, 7, 9, 18, 21, 22].

The middle third is the least problematic. Even on CT alone, a relatively low mean SD and coefficient of variance

Table 4. Intramodality interobserver mean standard deviation (and % decrease) of prostatic margin positions.

Tabelle 4. Mittlere Intramodalitäts-Interobserver-Standardabweichung (und prozentuale Abnahme) der Prostatarandpositionen.

	Anterior			Posterior			Right			Left			Superior/inferior		
	CT	MRI	%	CT	MRI	%	CT	MRI	%	CT	MRI	%	CT	MRI	%
Basal third	3.20	2.00	37.96*	2.20	1.60	27.85*	2.10	1.10	49.26*	1.40	1.30	10.96	2.10	1.60	23.36
Middle third	1.90	1.60	16.41*	2.00	1.70	14.74*	2.10	1.00	50.91*	1.70	1.00	39.25*	–	–	–
Apical third	2.00	1.60	18.90	2.30	1.40	41.41*	2.80	1.50	46.39*	2.60	1.40	46.58*	4.40	2.20	51.18*

*significance at $p < 0.05$ (paired t-test)

and a low uncertainty ratio are found. Because of the presence of fatty tissue around the prostate, the prostatic margin may be clearly visible on CT, where low-density fat contrasts well with intermediate-density prostatic tissue. This is illustrated by the relatively low mean SD around the mean position of the midprostatic borders (Table 4). However, fat may not be sufficiently present in all patients, especially at the posterior boundary with the rectum and the anterior boundary with Retzius' space, which may be vague due to the presence of adjoining intermediate-density veins of Santorini's venous plexus [9]. Because of a better contrast between the prostatic and surrounding tissues, the addition of MRI results in a significant, although small, decrease of the mean delineated volume and, more importantly, an improvement of the delineation accuracy, as demonstrated by a decrease of the mean SD around both the mean midprostatic volume and the position of the midprostatic margins, especially the lateral borders.

The basal third behaves on CT quite similar as the middle third, due to the presence of fatty tissue around the prostate. However, just underneath the bladder, the anterolateral margins are more difficult to delineate because of partial volume averaging with the isodense overlying bladder wall (which runs obliquely through the scan plane) [7]. It is also very difficult to differentiate the posterior aspect of the basal third from the nearly isodense seminal vesicles. Because of a more apparent distinction between the isointense prostate and the hypointense bladder wall on the one hand and the hyperintense seminal vesicles on the other hand, the addition of MRI to CT results in a significant decrease of the SD around the mean basal third volume and of the SD around the anterior and posterior mean position of the basal third borders, corroborating earlier findings by Kagawa et al. [9]. Interestingly, MRI does not lead to a significant improvement of the cranial delineation accuracy, because the use of iodinated contrast material on CT already allowed excellent visibility of the prostate-bladder transition and therefore rather straightforward identification of the uppermost part of the prostatic base (unlike the situation at the prostatic apex).

Although the seminal vesicles are generally surrounded by fatty tissue, their delineation on CT can be cumbersome because of the presence of the isodense deferent ducts medially and multiple plexular veins laterally. Furthermore, the boundary between the distal seminal vesicles and the prostatic base may be undistinguishable, as discussed above. Therefore, the uncertainty ratio on CT is quite high. On MRI, the seminal vesicles are usually visible as paired grape-like pouches filled with high signal-intensity fluid, as opposed to the low signal-intensity deferent ducts that traverse along their craniomedial sides [3]. MRI can therefore better separate the seminal vesicles from the deferent ducts and helps to more accurately delineate the most cranial portion of the (fluid-filled) seminal vesicles. The resulting effect is a significant decrease in the mean seminal vesicle volume and an improvement of the delineation accuracy, as demonstrated by a significant decrease of the mean SD and uncertainty ratio.

Our results suggest that the main impact of the addition of MRI to CT is a decrease of the delineation variation, rather than a decrease of the variation of mean margin positions or mean volumes. The latter contrasts with the substantial volume differences up to 34% that have been reported by several authors [4, 9, 21, 22]. Nevertheless, a moderate variation of prostate volume can be associated with only minor differences of margin position, because the volume of a spheroid object depends on the radius cubed. As previously illustrated by Roach et al., a 3-mm increase in the radius of a sphere from 1.8 to 2.1 cm results in a > 50% increase in the volume from 24 to 39 ml [22]. On the other hand, we believe that these differences are also a reflection of the large delineation variation on CT, more specifically a multiinstitutional variation, in which the magnitude of the difference largely depends on the CT delineation practice in a given center. In our hospital, we have been using MRI in concordance reading with a radiologist for > 3 years and hence our observers had a prior knowledge derived from MRI about the most likely boundaries of the prostate and seminal vesicles. This is illustrated by the fact that the prostate volume in our most experienced observer was even smaller on CT than on MRI, contrary to what is commonly expected.

An important question that could be raised is to what extent the decrease in delineation variation might have been influenced by the cooperation of the same radiologist, who could have been able to remember previous delineations, thereby favoring a very low intraobserver variation on CT + MRI. Although we expected that this impact, if any, would have been equally true (but in the opposite direction) for each radiation oncologist, we chose to prevent any possible bias as much as possible, by using a randomized order of appearance of the

13 patient files per reading set and a delay of at least 1 month between reading of each set. Furthermore, all CTVs were delineated by a radiation oncologist, not the radiologist: he was solicited to give advise about the MR information (consensus reading), not to delineate. Our results further plead against the hypothesis that the decreased delineation variation would be primarily influenced by the cooperation of the same radiologist rather than the additional use of MRI. Otherwise, we would have expected small and very similar SDs and coefficients of variation around the means of delineated volumes (Table 1) and mean SDs of prostatic margin positions (Table 4) throughout the prostate gland on CT + MRI delineations. However, they were usually larger at the apical third than at the basal third, and smallest at the middle third. We would also have expected CT + MRI delineation uncertainty indices converging to 1. Again, this was not the case (Table 2), suggesting that differences were determined by (MRI-based) anatomy, not by personal delineation consistency.

The clinical implication of a reduced variation of organ delineation with the addition of MRI in consensus with a radiologist is obvious. In a previous study, we showed that random prostatic movement as measured at the midprostatic level was 2.3 mm anteriorly, 3.2 mm posteriorly, 1.5 mm on the right side and 1.1 mm on the left side and 2.6 mm at the prostatic base and apex (all values representing 1 SD) [26]. From the present study, we conclude that the delineation variabilities on CT exceed those of the random prostatic movement variabilities (except the posterior and cranial margins), and that they significantly decrease when using MRI in addition to CT, reaching values of only half the random variation. As a result, the planning target volume can be decreased, resulting in an equal tumor control probability but a lower risk of complications.

References

1. Algan O, Hanks G, Shaer A. Localization of the prostatic apex for radiation treatment planning. Int J Radiat Oncol Biol Phys 1995;33:925–30.
2. Chism DB, Horwitz EM, Hanlon AL, et al. Late morbidity profiles in prostate cancer patients treated to 79–84 Gy by a simple four-field coplanar beam arrangement. Int J Radiat Oncol Biol Phys 2003;55:71–7.
3. Coakley F, Hricak H. Radiologic anatomy of the prostate gland: a clinical approach. Radiol Clin North Am 2000;38:15–30.
4. Debois M, Oyen R, Maes F, et al. The contribution of magnetic resonance imaging to the three-dimensional treatment planning of localized prostate cancer. Int J Radiat Oncol Biol Phys 1999;45:857–65.
5. De Meerleer G, Vakaet L, De Gersem W, et al. Direct segment aperture and weight optimization for intensity-modulated radiotherapy of prostate cancer. Strahlenther Onkol 2004;180:136–43.
6. De Meerleer GO, Villeirs GM, Vakaet L, et al. The incidence of inclusion of the sigmoid colon and small bowel in the planning target volume in radiotherapy for prostate cancer. Strahlenther Onkol 2004;180:573–81.
7. Fiorino C, Reni M, Bolognesi A, et al. Intra- and inter-observer variability in contouring prostate and seminal vesicles: implications for conformal treatment planning. Radiother Oncol 1998;47:285–92.
8. Geinitz H, Zimmermann F, Wedel E von, et al. Biochemical control after conformal, 3-dimensional radiotherapy of prostatic carcinoma. Strahlenther Onkol 2002;178:369–77.
9. Kagawa K, Lee W, Schultheiss T, et al. Initial clinical assessment of CT-MRI image fusion software in localization of the prostate for 3D conformal radiation therapy. Int J Radiat Oncol Biol Phys 1997;38:319–25.
10. Karlsdottir A, Johannessen DC, Muren LP, et al. Acute morbidity related to treatment volume during 3D-conformal radiation therapy for prostate cancer. Radiother Oncol 2004;71:43–53.
11. Khoo V, Dearnaley D, Finnigan D, et al. Magnetic resonance imaging (MRI): considerations and applications in radiotherapy treatment planning. Radiother Oncol 1997;42:1–15.
12. Khuntia D, Reddy CA, Mahadevan A, et al. Recurrence-free survival rates after external-beam radiotherapy for patients with clinical T1–T3 prostate carcinoma in the prostate-specific antigen era: what should we expect? Cancer 2004;100:1283–92.
13. Koelbl O, Schwab F, Bratengeier K, et al. Radiotherapy of prostate cancer with multileaf collimators (MLCs). Optimization of the undulating dose distribution at the MLC edge. Strahlenther Onkol 2005;181:108–12.
14. Kuban D, Pollack A, Huang E, et al. Hazards of dose escalation in prostate cancer radiotherapy. Int J Radiat Oncol Biol Phys 2003;57:1260–8.
15. Lee YK, Bollet M, Charles-Edwards G, et al. Radiotherapy treatment planning of prostate cancer using magnetic resonance imaging alone. Radiother Oncol 2003;66:203–16.
16. Luxton G, Hancock SL, Boyer AL. Dosimetry and radiobiologic model comparison of IMRT and 3D conformal radiotherapy in treatment of carcinoma of the prostate. Int J Radiat Oncol Biol Phys 2004;59:267–84.
17. Michalski JM, Winter K, Purdy JA, et al. Toxicity after three-dimensional radiotherapy for prostate cancer with RTOG 9406 dose level IV. Int J Radiat Oncol Biol Phys 2004;58:735–42.
18. Milosevic M, Voruganti S, Blend R, et al. Magnetic resonance imaging (MRI) for localization of the prostatic apex: comparison to computed tomography (CT) and urethrography. Radiother Oncol 1998;47:277–84.
19. Nunes LW, Schiebler MS, Rauschning W, et al. The normal prostate and periprostatic structures: correlation between MR images made with an endorectal coil and cadaveric microtome sections. AJR Am J Roentgenol 1995; 164:923–7.
20. Pollack A, Hanlon AL, Horwitz EM, et al. Prostate cancer radiotherapy dose response: an update of the fox chase experience. J Urol 2004;171:1132–6.
21. Rasch C, Barillot I, Remeijer PK, et al. Definition of the prostate in CT and MRI: a multi-observer study. Int J Radiat Oncol Biol Phys 1999;43:57–66.
22. Roach MR, Faillace-Akazawa P, Malfatti C, et al. Prostate volumes defined by magnetic resonance imaging and computerized tomographic scans for three-dimensional conformal radiotherapy. Int J Radiat Oncol Biol Phys 1996;35:1011–8.
23. Sanguineti G, Castellone P, Foppiano F, et al. Anatomic variations due to radical prostatectomy. Impact on target volume definition and dose-volume parameters of rectum and bladder. Strahlenther Onkol 2004;180:563–72.
24. Scharma R, Duclos M, Chuba PJ. Enhancement of prostate tumor volume definition with intravesical contrast: a three-dimensional dosimetric evaluation. Int J Radiat Oncol Biol Phys 1997;38:575–82.
25. Symon Z, Griffith KA, McLaughlin PW, et al. Dose escalation for localized prostate cancer: substantial benefit observed with 3D conformal therapy. Int J Radiat Oncol Biol Phys 2003;57:384–90.
26. Villeirs GM, De Meerleer GO, Verstraete KL, et al. MR-assessment of prostate localization variability in intensity-modulated radiotherapy for prostate cancer. Int J Radiat Oncol Biol Phys 2004;60:1611–21.
27. Zelefsky MJ, Fuks Z, Hunt M, et al. High dose radiation delivered by intensity-modulated conformal radiotherapy improves the outcome of localized prostate cancer. J Urol 2001;166:876–81.

Address for Correspondence
Geert M. Villeirs, MD
Department of Radiology
Ghent University Hospital
De Pintelaan 185
9000 Gent
Belgium
Phone (+32/9) 240-3108, Fax -4976
e-mail: Geert.Villeirs@ugent.be